https://doi.org/10.5194/amt-2023-65
Preprint. Discussion started: 25 April 2023

Atmospheric Measurement Techniques
Discussions

Spring and summertime aerosol optical depth retrieval over the Arctic cryosphere by using satellite observations

Basudev Swain[1], Marco Vountas[1], Adrien Deroubaix[1,3], Luca Lelli[1,2], Yanick Ziegler[1,4], Soheila Jafariserajehlou[1,6], Sachin S. Gunthe[5], and John P. Burrows[1]

[1]Institute of Environmental Physics, University of Bremen, Germany
[2]Remote Sensing Technology Institute, German Aerospace Centre (DLR), Wessling, Germany
[3]Max-Planck-Institut für Meteorologie, Hamburg, Germany
[4]now with Karlsruhe Institute of Technology, Institute of Meteorology and Climate Research-Atmospheric Environmental Research (KIT/IMK-IFU), Garmisch-Partenkirchen, Germany
[5]Indian Institute of Technology Madras, Chennai, India
[6]now with EUMETSAT/Rhea Group, Germany

Correspondence: Basudev Swain (basudev@iup.physik.uni-bremen.de)

Abstract.

The Arctic climate has changed significantly over the past two to three decades. Aerosols play various roles in the radiative forcing in the Arctic, both directly and indirectly, depending on the changes in loading and composition. However, their observation from the ground or with airborne instruments is challenging and thus measurements are sparse. In this study, total Aerosol Optical Depth (AOD) is determined from top-of-atmosphere reflectance measurements by the Advanced Along-Track Scanning Radiometer (AATSR) aboard ENVISAT over snow and ice in the Arctic using a retrieval called AEROSNOW for the period 2003 to 2011. We use the dual-viewing capability of the AATSR instrument to reduce the impact of surface reflectance on the accuracy of AOD. The AOD is retrieved assuming that the surface reflectance observed by the satellite can be well-parametrized by a bidirectional snow reflectance distribution function, BRDF. The spatial distribution of AODs shows that high values in spring (March, April, May) and lower AOD values in summer (June, July, August) are well captured. Spaceborne AOD values are consistent with colocated AERONET measurements, with no systematic bias as a function of time. The AEROSNOW AOD in the high Arctic ($\geq$ 72°N) was validated by comparison with ground-based measurements at the PEARL, OPAL, Hornsund, and Thule stations. The AEROSNOW AOD value is less than 0.15 on average and the regression to AERONET yields a slope of 0.98, a Pearson correlation coefficient of R = 0.86, and an RMSE = 0.01 at a monthly scale, both in spring and summer. These AOD results provide, for the first time, observational insights into the central Arctic with significant spatial and temporal coverage.

1 Introduction

The Arctic has experienced a significant increase in near-surface air temperatures over the past three decades: the rate of temperature increase being about two to three times larger than the global mean. This phenomenon is known as Arctic Amplification (AA) (Serreze and Francis, 2006). The warming of the Arctic has increased the rate of melting of the Arctic cryosphere,

https://doi.org/10.5194/amt-2023-65
Preprint. Discussion started: 25 April 2023

Atmospheric Measurement Techniques Discussions

e.g. glaciers, sea ice, and snow-covered surfaces. Processes thought to influence AA include for example the following: surface albedo feedback (Perovich and Polashenski, 2012), warm air intrusion (Boisvert et al., 2016), and oceanic heat transport (Nummelin et al., 2017), cloud feedback (Kapsch et al., 2013; He et al., 2019; Middlemas et al., 2020), lapse rate feedback (Pithan and Mauritsen, 2014), and biological and oceanic particle emission effects (Park et al., 2015; Campen et al., 2022).

Atmospheric aerosols are a collection of solid or liquid suspended particles that have both natural and anthropogenic sources. It is well known that changes in the scattering and absorption of incoming solar radiation by aerosols have a direct impact on climate change (Bond et al., 2013). Increases in aerosol result in more solar radiation being scattered back into space and the atmosphere and surface are cooled. On the other hand, aerosols that absorb solar radiation warm the atmosphere and surface. Aerosols also act as both cloud condensation nuclei (CCN) and ice nuclei (IN), affecting the microphysical and radiative properties of clouds. In this way, aerosols also indirectly affect climate change (Twomey, 1977; Kaufman and Fraser, 1997; Hartmann et al., 2020). However, neither the contribution of aerosols to AA nor the effect of declining regional snow and ice on aerosol during the AA period is well understood (Im et al., 2021).

In this study we use the Aerosol Optical Depth (AOD) as an optical measure of aerosol. It is valuable in the analysis of the impact of aerosols on the Arctic climate and vice versa. The retrieval of AOD is complicated by the seasonal changes of solar geometry, surface albedo, and meteorology (Mei et al., 2013, 2020a; Stapf et al., 2020). The AOD is defined as the columnar integration of the aerosol extinction coefficient (the sum of the absorption and scattering coefficient).

The Arctic is vast and the ground-based measurements of AOD are inevitably sparse. This has limited our understanding of the direct and indirect impact of aerosols on AA, and vice versa. Recently there have been some campaigns, which have investigated different processes of relevance to aerosol sources and sinks in the Arctic e.g. MOSAiC campaign (https://mosaic-expedition.org), ACLOUD/PASCAL (Wendisch et al., 2019), PAMARCMIPs (Hoffmann et al., 2012; Nakoudi et al., 2018; Ohata et al., 2021). In addition, there are other site-based long-term aerosol measurement studies (Herber et al., 2002; Tomasi et al., 2007; Moschos et al., 2022; Schmale et al., 2022). However, these provide an inadequate spatiotemporal representation of the Arctic region (Sand et al., 2017). The sparseness of AOD may explain, at least in part, the variations of AOD simulations from different climate models (Sand et al., 2017). Without doubt, the lack of AOD measurements in the Arctic limits our knowledge about radiative forcing and the Arctic warming in global and regional climate models (Goosse et al., 2018).

Further, AOD has been retrieved from the measurements of reflectance at Top-Of-Atmosphere (TOA), made by passive satellite remote sensing instrumentation over the Arctic, but almost exclusively over snow- and ice-free areas i.e. land and ocean. A few recent studies have used such AOD products (e.g., (Glantz et al., 2014; Wu et al., 2016; Sand et al., 2017; Xian et al., 2021)) over open ocean and snow- and ice free surfaces, and make a valuable contribution to closing the data gap mentioned above. However, these AOD products are not suitable over the cryosphere due to an inadequate parameterization of the surface reflectance over residual snow- and ice-covered areas (Mei et al., 2020a) and Arctic cloud cover (Jafariserajehlou et al., 2019). In addition, typical illumination conditions, i.e. large solar zenith angles make the AOD retrieval used in the Arctic more challenging and lead potentially to a significant overestimation of AOD values (Mei et al., 2013).

Several dedicated algorithms for passive satellite remote sensing over snow and ice have been developed. (Istomina et al., 2011) and later (Mei et al., 2013, 2020b, a) have provided valuable pioneering research. However, these attempts have been mostly confined to the island of Spitsbergen in the Svalbard archipelago in northern Norway. Thus far, there have been no attempts to apply these algorithms systematically in the Arctic cryosphere to fill the data gap, identified above. Studies using active satellite remote sensing such as Sand et al. (2017) and Xian et al. (2021) are valuable, but the observational data are limited over the Arctic cryosphere.

Recently, Toth et al. (2018) and Xian et al. (2021) reported that the active satellite sensor, the Cloud-Aerosol Lidar with Orthogonal Polarization (CALIOP/CALIPSO) (Winker et al., 2004) has a significant fraction of aerosol profile data consisting of retrieval fill values (-9999s, or RFVs), due in part to the lidar's minimum detection limits. Indeed, in some areas in the Arctic, over 80% of CALIOP profiles consist solely of RFVs.

Consequently, the objective of this study is to retrieve the AOD over snow- and ice-covered regions of the Arctic. In this way, we extend the retrieval of aerosol loading over polar regions because past efforts, using the same AATSR source data, did not cover the high latitudes (Popp et al., 2016). To achieve this goal, we retrieve the total AOD using an approach first described by (Istomina et al., 2011), which we have further developed and named AEROSNOW. We assessed the quality of AEROSNOW by using Aerosol Robotic Network (AERONET) measurements to validate the retrieved AOD.

We have generated the AEROSNOW AOD data set for the period from 2003 to 2011 (9 years). The algorithm uses the measurements, made by the Advanced Along-Track Scanning Radiometer (AATSR) data over the Arctic. A short description of the AATSR data and the corresponding retrieval is given in section 2. To determine the quality of the AEROSNOW data sets, we compare them with accurate ground-based AERONET measurements in the high Arctic. The description of the AERONET dataset is found in section 2.2. The AERONET and AEROSNOW values are then compared at selected high latitude AERONET stations over snow and ice-covered surfaces in section 3. Finally, we draw conclusions in section 4.

2 Data Sets and Data Processing

To investigate the distribution and variability of Arctic aerosols over snow and ice, we have used passive remote sensing during spring (March, April, April, May, (MAM)) and summer (June, July, August, (JJA)), which is the time when the Arctic is illuminated by solar radiation. The AEROSNOW algorithm is applied to the dual view Level 1B data product reflectance at the top of the atmosphere made by AATSR (Llewellyn-Jones et al., 2001). We have validated the AEROSNOW AOD retrieved by comparing with AOD, measured by the ground-based sun-photometer measurements, AERONET (Holben et al., 1998).

2.1 Satellite Retrieval

2.1.1 AATSR Instrument

The AATSR flew, as part of the payload of the European Space Agency's (ESA) ENVISAT, which was launched on 28.02.2002 and failed on 08.04.2012. ENVISAT flew in a sun-synchronous orbit with an equatorial crossing local time of 10 o'clock.

https://doi.org/10.5194/amt-2023-65
Preprint. Discussion started: 25 April 2023

AATSR made measurements from May 2002 to April 2012. The spatial resolution of the AATSR observation data was 1 km at nadir. The swath width of AATSR was 512 km. AATSR had a dual viewing capability with a forward viewing angle of 55°. It made simultaneous measurements of the upwelling reflectances at wavelengths, from the visible to thermal infrared (0.55, 0.66, 0.87, 1.6, 3.7, 11, and 12 μm).

2.1.2 AEROSNOW Algorithm

The dual-viewing capability of the AATSR instrument was exploited to retrieve AOD over snow and ice using the AEROSNOW algorithm. AEROSNOW comprises a cloud identification routine or, cloud mask and an algorithm to determine the AOD for cloud free scenes. For the cloud mask, we adapted the implementation of the approach proposed in (Jafariserajehlou et al., 2019). The AATSR-SLSTR cloud identification algorithm (ASCIA) meets the requirements for the high-latitude AOD study and uses a dedicated set of thresholds for radiation and time-series measurements. Cloud-free surfaces are assumed to exhibit unchanged or only slightly changed patterns for a given sampling period, while cloudy or partly cloudy scenes show much higher variability in space and time. For more information, such as thresholds and channels used, the reader is referred to the schematic flow chart of the cloud identification algorithm shown in Fig. 4 of the article by Jafariserajehlou et al. (2019).

For the selected cloud free scenes, the AOD is then retrieved. Instead of computational time-intensive online calculations a look up table (LUT) approach is used in the retrieval. The LUT contains AOD for values of the solar zenith angle θ, and relative azimuth angle ϕ. The method uses the ratio of the reflectance for nadir and forward observations (the dual-view), measured at TOA. A forward radiative transfer model SCIATRAN (Rozanov, 2001; Rozanov et al., 2002, 2005) simulates the values of this ratio. An analytical solution for the BRDF of snow (Kokhanovsky and Breon, 2012), as well as tabulated values of transmissivity (from look-up tables) were used in an iterative procedure to obtain the AOD over Arctic snow and ice regions at 555 nm.

The algorithm takes advantage of the ability of the AATSR instrument to observe in two different viewing directions. It was described in Istomina et al. (2011). Consequently, we now provide only a short overview of this algorithm. The reflectance of the surface can be approximated by two terms. One term describes the dependence of the reflectance on the wavelength and the other describes the dependence of reflectance on the viewing geometry The surface reflectance ratio is mainly determined by the shape and magnitude of the surface BRDF (Vermote et al., 1997). This reduces the need for a highly accurate simulation of the wavelength-dependent surface reflectance, which is useful for bright surfaces such as snow- or ice-covered regions (Vermote et al., 1997).

We need to separate accurately the surface reflectance from the atmospheric contributions. Therefore, a suitable snow BRDF model is needed that depends on the viewing and illumination angle, wavelength, and snow properties such as size and shape of grains and characterizes both AATSR observation directions. The BRDF model is analytical and was compared with a series of multispectral and multidirectional measurements from the POLDER-3 (Polarization and Directionality of the Earth's Reflectances) instrument aboard the PARASOL satellite (Polarization and Anisotropy of Reflectances for Atmospheric Sciences coupled with Observations from a Lidar). We fixed the free parameters for the entire time series of AATSR, which involved a fixed snow grain size and snow impurity assumptions.

A snow BRDF model was selected as follows (Kokhanovsky and Breon, 2012):

$$\rho(\mu,\mu_0,\phi) = R_0(\mu,\mu_0,\phi)A^{f(\mu,\mu_0,\phi)}$$

where

$$A = exp\left(\frac{-4s}{\sqrt{3}}\right), s = \sqrt{\frac{1-\omega}{1-g\omega'}}$$

$$f = \frac{u(\mu)u(\mu_0)}{R_0(\mu,\mu_0,\phi)}$$

$$u(\mu) = \frac{3}{7}(1+2\mu)$$

$$R_0(\mu,\mu_0,\phi) = \frac{a+b(\mu+\mu_0)+c\mu\mu_0+p(\theta)}{4(\mu+\mu_0)}$$

where $R_0(\mu,\mu_0,\phi)$ is the reflection function for non-absorbing snow layer, $\mu = \cos\theta$ and $\mu_0 = \cos\theta_0$, θ_0 and θ are solar zenith angle and satellite zenith angle, g is the asymmetry factor of snow particle, ω is the single scattering albedo, $a = 1.247$, $b = 1.186$, $c = 5.157$, ϕ is the azimuth angle, $p(\theta) = 11.1\exp(-0.087\theta) + 1.1\exp(-0.014\theta)$, respectively.

Istomina et al. (2011) used the following Eq. to mitigate atmospheric effects by introducing modelled $\rho_{\text{sfc,sim}}(\lambda,\mu_0,\mu,\phi)$ and $\rho_{\text{TOA,sim}}(\lambda,\mu_0,\mu,\phi)$ ratios of forward and nadir view:

$$\frac{\rho^f_{\text{sfc}}(\lambda,\mu_0,\mu,\phi)}{\rho^n_{\text{sfc}}(\lambda,\mu_0,\mu,\phi)} = \frac{\rho^f_{\text{sfc,sim}}(\lambda,\mu_0,\mu,\phi)}{\rho^n_{\text{sfc,sim}}(\lambda,\mu_0,\mu,\phi)} \frac{\rho^n_{\text{TOA,sim}}(\lambda,\mu_0,\mu,\phi)}{\rho^f_{\text{TOA,sim}}(\lambda,\mu_0,\mu,\phi)} \frac{\rho^f_{\text{TOA}}(\lambda,\mu_0,\mu,\phi)}{\rho^n_{\text{TOA}}(\lambda,\mu_0,\mu,\phi)} \quad (1)$$

where $\rho_{\text{sfc}}(\lambda,\mu_0,\mu,\phi)$ is the surface reflectance, $\rho_{\text{TOA}}(\lambda,\mu_0,\mu,\phi)$ is the satellite observed TOA reflectance, λ is the wavelength, and f and n indicate AATSR forward and nadir observation angles, respectively.

An important aerosol property is the aerosol phase function. In this work, two types of aerosols were used: one is a background aerosol and the other is Arctic haze. The phase functions for these two types are shown in Istomina et al. (2011). The Arctic haze aerosol was measured during the Arctic haze event at Spitsbergen (78.923N, 11.923E) on March 23, 2003. Subsequently, the look-up table was calculated using the SCIATRAN radiative transfer package (Rozanov et al., 2014; Mei et al., 2023).

2.2 AERONET Level 2 Aerosol Product

The AErosol RObotic NETwork, AERONET, is a federated network of ground-based global sun photometers measuring solar and sky irradiance at various wavelengths from the near ultraviolet to the near infrared with high accuracy (Holben et al., 2001; Giles et al., 2019). AERONET sun photometers record AOD values every 15 minutes in typically seven spectral channels

https://doi.org/10.5194/amt-2023-65
Preprint. Discussion started: 25 April 2023

Atmospheric Measurement Techniques Discussions

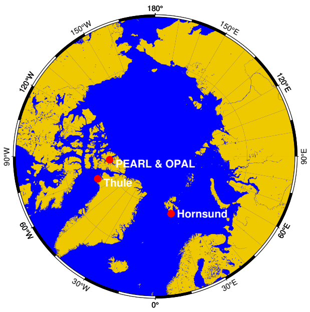

Figure 1. Location of PEARL, OPAL, Hornsund and Thule AERONET measurement stations considered in this study.

(nominally 340, 380, 440, 500, 670, 870, and 1020 nm) (Holben et al., 2001). The quality-assured AERONET version 3 level 2 data are used in this study (accessed at http://aeronet.gsfc.nasa.gov).

The AOD from AERONET stations in the high Arctic were used to assess the data quality of AOD estimated using AEROSNOW. The locations of the AERONET stations selected are PEARL (80.054N, 86.417W), OPAL (79.990°N, 85.939°W), Hornsund (77.001°N, 15.540°E) and Thule (76.516°N, 68.769°W) and shown in Fig. 1. Two sites are located over the Canadian archipelago (CA), which typically has aerosol of natural origin (Breider et al., 2017) and one station Hornsund on Spitsbergen, which is known to be affected by polluted air masses from lower latitudes.

2.3 Data quality control

To compare the AOD of AERONET measured at 500 nm with those of AEROSNOW (measured at 555 nm), a conversion is required. The AOD at 500 nm is used to extrapolate the AOD at 555 nm by using 500-870 nm Angstrom Exponent. In addition, the AOD at 555 nm is considered as the total AOD to allow comparison with the AEROSNOW data. AERONET observations were averaged and compared to values measured within a 25-km radius and 30-minute time collocation of the AERONET stations for AEROSNOW. Monthly averages were calculated based on the spatio-temporal colocated data. Information about the collocated daily values derived is shown in the appendix (Fig. A1).

In post-processing AEROSNOW, we selected optimal conditions, i.e. by using a cutoff value for the solar zenith angle ($\geq$ 75°) and filtering out those scenes or pixels that had a Normalized-Difference Snow Index (NDSI) $\leq$ 0.97. The NDSI is an index that refers to the presence of snow in a pixel and is a more accurate description of snow detection compared to fractional snow cover. Snow typically has a very high reflectance in the visible spectrum (VIS) and a very low reflectance in the shortwave infrared (SWIR). Snow coverage is determined by the NDSI ratio of the difference between the VIS and SWIR reflectance. A pixel with NDSI > 0.0 is considered to have snow present, while a pixel with NDSI $\leq$ 0.0 represents a snow-free land surface (Riggs et al., 2017). In this study, NDSI was used in a rigorous post-processing of the datasets to filter out the mixed and snow-free regions.

To ensure quality, we also noted that melt ponds and thin clouds not captured by rigid filtering deteriorate the retrieval quality of AEROSNOW. Recently Xian et al. (2021) introduced a post-processing scheme to remove erroneous AOD outliers. Instead of applying the rather qualitative quality flagging approach as proposed by the former, we applied a more quantitative one. We thoroughly examined the ratio of AEROSNOW to AERONET AOD greater than a factor of 1.6 by calculating a quality flag (QF) parameter [QF = (0.8 × (snow cover fraction) + 0.2 × (1 - cloud fraction)] which penalizes the low levels of snow cover and (and to less extent) residual cloud fraction by using MODIS Terra and Aqua data products from NASA Worldview (https://worldview.earthdata.nasa.gov/) respectively. When using the AEROSNOW data beyond the AERONET stations, we applied this scheme to all data points of AEROSNOW. Empirical tests showed that an appropriate snow cover fraction is weighted higher than an appropriate clear sky fraction (1 - cloud fraction). This is expressed by the individual weighting factors for snow cover fraction (0.8) and clear sky fraction (0.2). We found that a QF threshold value of 0.6 represents a compromise between data yield and data quality. Thus, in the final step, AOD values having a QF value of 0.6 or less were removed.

3 Result: Assessment of AEROSNOW AOD

3.1 Qualitative Analysis of AEROSNOW

Before we turn to quantitative validation of the AEROSNOW results, we discuss the spatio-temporal distribution of the AEROSNOW data here briefly in qualitative terms. The spatio-temporal frequency of observations over the Arctic from both ground and satellite is larger in summer (JJA) than in spring (MAM). Fig. 2 shows the monthly averaged AOD over snow and ice of the Arctic for the period 2003-2011, with significant differences in the spatial distribution of AOD. In this study, satellite retrievals are performed only when snow and ice are present (NDSI-threshold values, see section 2). The NDSI was used to constrain the BRDF in terms of snow grain size and impurity (when snow accumulation is fresh) and clouds are absent. Accordingly, the best coverage is obtained over persistently homogeneous areas covered with (fresh) snow and ice. Greenland is an exception to the AOD retrieval. Possible reasons for this could be that the BRDF does not fit well because it does not adequately represent the snow grains and impurities of the Greenland glaciers and snow covered ice sheet and the elevated topography. Further, the clouds over Greenland are typically optically thin and low-hanging (Bennartz et al., 2013) and are likely not all captured by the ASCIA cloud detection algorithm. Smoother patterns are observed in Fig. 2 over the Arctic sea ice compared to snow-covered land.

3.2 Statistical evaluation of AODs from AERONET and AEROSNOW

The satellite retrieved and ground based observations are compared. Uncertainties due to both space and time sampling differences are minimized. Fig. 3 shows the validation between AEROSNOW retrieved AOD over PEARL, OPAL, Hornsund and Thule, with AERONET AOD during this study period. Fig. A1 in the appendix depicts daily collocated values and statistics.

Much of the data analysis in this paper involves fitting a straight line to the AODs observed by both AERONET and AEROSNOW. Because the AOD observations by these two platforms are both subject to measurement errors (Sinyuk et al., 2012; Mei et al., 2013), we have used a fitting procedure known as the reduced major axis (RMA) method, as described by Hirsch and

Gilroy (1984); Ayers (2001). These authors concluded that the RMA method is more appropriate than ordinary Least Squares regression because the latter does not take into account the relationships between geophysical variables. The RMA takes account of random variance in both the x and y variables, rather than solely in the y variable. Therefore, it is recommended that the use of reduced major axis (RMA) regression replace the use of standard linear regression. RMA has been used by other researchers in the analysis of air quality and atmospheric chemistry data see for example Keene et al. (1986); Arimoto et al. (1995); Freijer and Bloemen (2000); Ayers (2001); Wang et al. (2004)

By combining these four stations, the coefficient of correlation (R) is on average 0.86 and the root mean square error (RMSE) is 0.01. Validating each stations separately the R value is increasing to 0.90, 0.94, 0.81 and 0.87 over PEARL, OPAL, Hornsund and Thule respectively (Fig. 4). We consider R values of about 0.8 to be sufficient under the Arctic condition that these are exceptionally challenging retrievals.

3.3 Comparison of AODs from AERONET and AEROSNOW

In the next step, we analyze the colocated temporal evolution of the AEROSNOW results and compare with AERONET station data. The time-series of retrieved AEROSNOW AOD is shown together with AERONET data in Fig. 5. In general, the time-series for AERONET is well reproduced by AEROSNOW.

In general and as expected, we observe that PEARL, OPAL and Thule (extended Canadian archipelago, henceforth called CA-stations) exhibit similar temporal behavior. PEARL and OPAL AERONET sites are located around 11.5 km apart. OPAL is closer to the coast than PEARL station and are located at altitudes of 5.0 m and 615.0 m, respectively. Hornsund is in this context clearly different. This difference can be explained by using an optimal chemical transport model by separating the total AOD to aerosol components.

The CA-stations show low average values AOD. This is associated with Arctic background scenarios. The seasonal variability over all these three stations are presented Fig. 6, which shows that both the AEROSNOW and AERONET results exhibit higher AOD during spring (MAM) and minimum during summer (JJA). A partially high estimation of AEROSNOW is observed over all the selected sites in August, which may be due to uncertainties in surface parameterization and aerosol types in this region.

On average, AEROSNOW appears to capture some haze events during spring and thereby has higher average values than in the summer season.

3.4 Spring and Summertime AOD over the Arctic Sea Ice

Similar to the analysis shown in Fig. 5, where we examined the time series of total AOD from AEROSNOW over AERONET stations, we now discuss qualitatively how AOD values change over time across the entire region of Arctic sea ice. The combination of seven AATSR channels was used to distinguish the spectral response of a clear snow-covered landscape from that of clouds, land, and sea. For more details on the procedure to distinguish between snow-covered areas and land, open sea areas, etc., see the explanation and Eq.s 4, 5, and 6 in Istomina et al. (2011).

https://doi.org/10.5194/amt-2023-65
Preprint. Discussion started: 25 April 2023

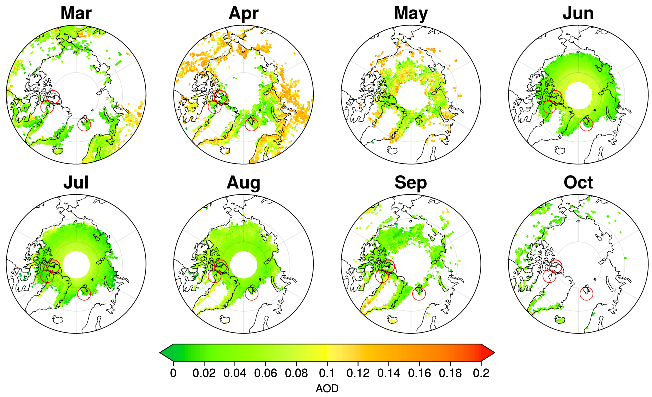

Figure 2. Pan-Arctic seasonal view of AEROSNOW retrieved AOD over snow and ice averaged from the year 2003 to 2011 for the months March to October, thus large parts of the period of insolation. Red circles indicate the location of AERONET stations.

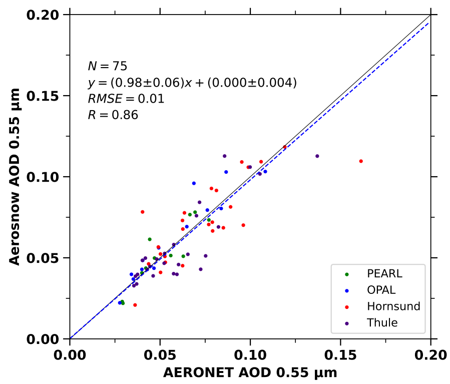

Figure 3. Validation of monthly mean AEROSNOW retrieved AOD colocated with monthly mean AERONET observation AOD obtained over PEARL, OPAL, Hornsund, and Thule stations. The linear regression line are shown as the blue dashed line.

The AEROSNOW AOD results over pan-Arctic sea ice shown in Fig. 8, exhibit maximum values in spring 2009 and minimum values in spring 2006. However, comparing the seasonally averaged climatology from 2003 to 2011, the AEROSNOW results indicate higher AOD in the spring, and smaller values in summer (Fig. 9) which was expected.

On the other hand, the AEROSNOW retrievals of AOD may be affected by cloud contamination because high levels of cloud cover are observed over the Arctic in summer with average values around 0.8 (Kato et al., 2006). Although we adopted reasonable cloud masking for the AOD retrievals, we cannot exclude entirely the possibility that residual cloud contamination prevails (Jafariserajehlou et al., 2019).

Additionally, AEROSNOW captures the higher values of AOD over north Alaska and Siberia during summer, a region which is often influenced by boreal forest fires during this period (Xian et al., 2021) (Fig. 7). During spring the higher values of AOD (0.1-0.12) are observed near Europe and the Asian continent and smaller values (0.07-0.08) towards CA. Spring values are

https://doi.org/10.5194/amt-2023-65
Preprint. Discussion started: 25 April 2023

Atmospheric Measurement Techniques
Discussions

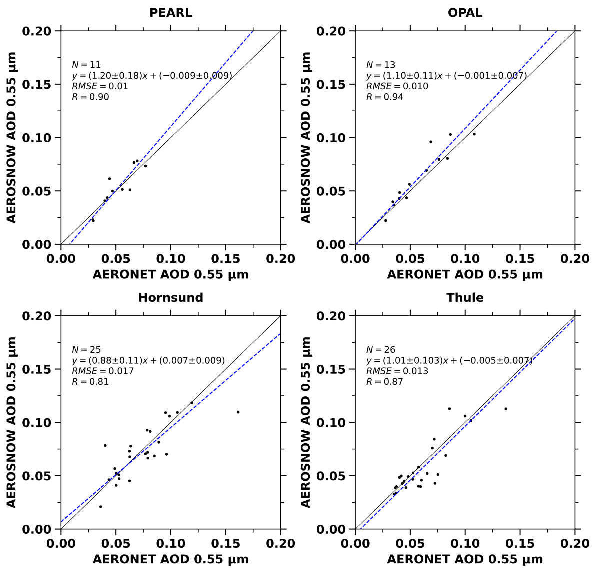

Figure 4. Validation of monthly mean AEROSNOW retrieved AOD colocated with monthly mean AERONET observation AOD obtained over PEARL, OPAL, Hornsund, and Thule stations. The linear regression lines are shown as blue dashed line.

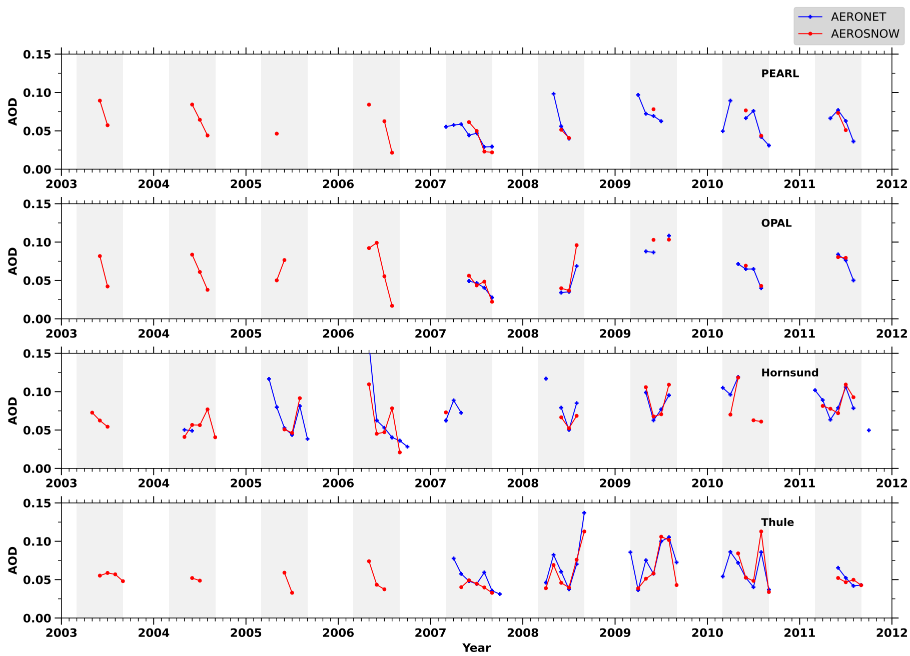

Figure 5. Monthly mean time-series of AERONET and AEROSNOW AOD at PEARL, OPAL, Hornsund, and Thule stations. The MAM,JJA periods are highlighted with light-grey shades.

https://doi.org/10.5194/amt-2023-65
Preprint. Discussion started: 25 April 2023

Atmospheric Measurement Techniques
Open Access
EGU
Discussions

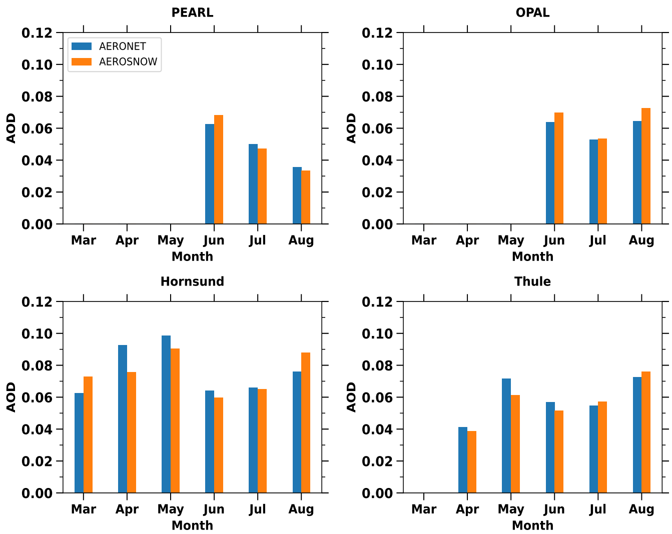

Figure 6. Seasonal AOD variation over PEARL, OPAL, Hornsund and Thule with AEROSNOW and AERONET values average from 2003 to 2011. Blue and orange bar plots shows statistics for AERONET and AEROSNOW respectively.

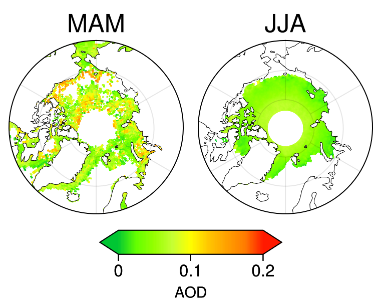

Figure 7. Mean climatological MAM and JJA AEROSNOW derived AOD over Arctic Sea Ice averaged from the year 2003 to 2011. White area shows lack of data apart from the masked land area.

mostly dominated by long-range transport of anthropogenic aerosols from the lower latitudes of Europe, America, and Asia (Willis et al., 2018). The AEROSNOW estimates of AOD over central Arctic sea ice are reasonable and thus a valuable source to fill the aerosol data deficit over the perennial sea ice region in the high Arctic.

The comparison of the AEROSNOW data with model data is the next logical step. We test the quality and limitations of the model as well as of the satellite dataset in the high Arctic. Further, the seasonal variability of AOD observed from AEROSNOW can then be attributed by investigating aerosol properties, components, long-range transport, and local sources. This is possible by using an optimal chemical transport model with updated emission inventories for this study period.

https://doi.org/10.5194/amt-2023-65
Preprint. Discussion started: 25 April 2023

Atmospheric Measurement Techniques
Discussions

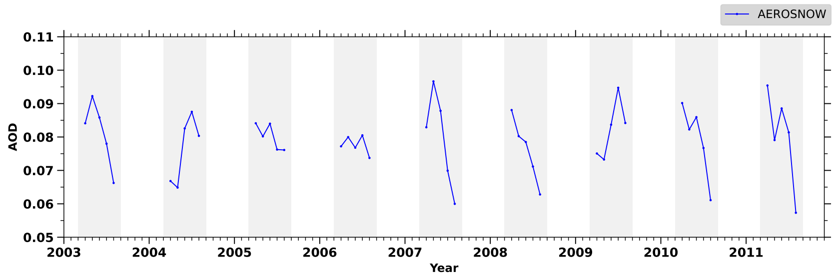

Figure 8. Monthly mean time-series of AEROSNOW AOD over Arctic sea-ice region. The MAM,JJA periods are highlighted with light-grey shades.

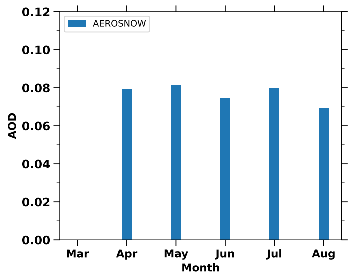

Figure 9. Seasonal AOD variation over Arctic sea-ice region values averaged from 2003 to 2011. Blue bars denote observed monthly mean AODs of AEROSNOW respectively.

4 Conclusions

This is the first time that AOD has been determined using satellite data over the entire Arctic snow and ice surface over a nine-year period and validated with ground based AERONET measurement. A satellite-based retrieval of AOD over Arctic snow and ice (AEROSNOW, (Istomina et al., 2011)) was conducted, which has been shown to fill the gap in data availability from standard aerosol products such as e.g. MODIS. The AEROSNOW algorithm uses the dual-viewing capability of the AATSR instrument to minimize retrieval uncertainties. It showed good agreement with ground-based AERONET observations, with a correlation coefficient R = 0.86 and a low systematic bias. The high anthropogenic aerosol loading (Arctic haze events) due to long-range transport over Arctic snow and ice is captured by the AOD determined by AEROSNOW. The time series and seasonality of the AEROSNOW AOD agree well with AERONET observations. Good agreement between the AEROSNOW and AERONET AOD is achieved over PEARL, OPAL, Hornsund, and Thule stations. The AEROSNOW retrieved AOD shows maximum values during spring (MAM) and minimum during summer (JJA), which is also in accordance with AERONET measurements. Further improvement of the AOD retrieval could be possible in terms of cloud masking, surface reflectivity properties, and the adoption of more appropriate aerosol types to be considered.

https://doi.org/10.5194/amt-2023-65
Preprint. Discussion started: 25 April 2023

The promising AOD results obtained with AEROSNOW indicate that these can be used to evaluate and improve aerosol predictions for various chemical transport models, especially over the Arctic sea ice in spring and summer for the important period 2003-2011, which is within the period of Arctic amplification.

https://doi.org/10.5194/amt-2023-65
Preprint. Discussion started: 25 April 2023

Atmospheric Measurement Techniques Discussions

Appendix A: Additional Figures

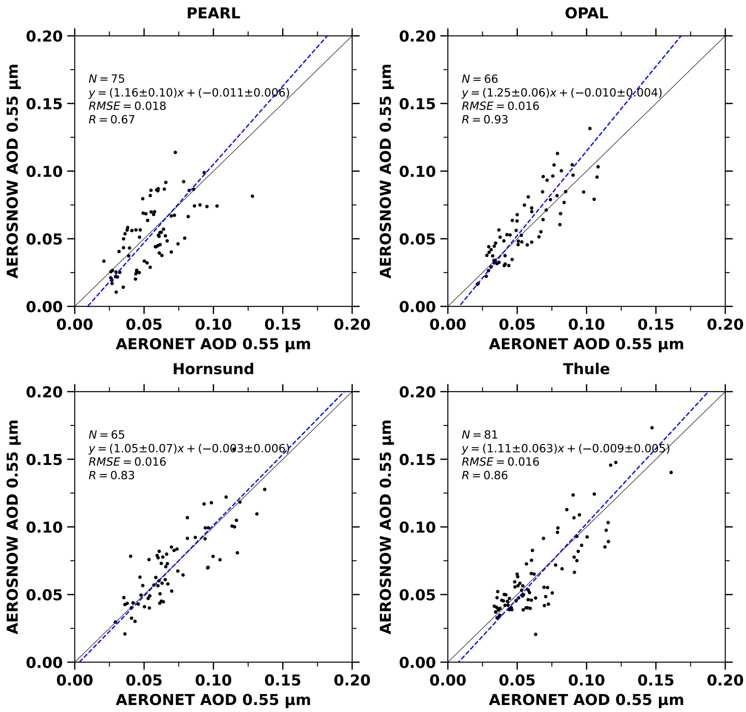

Figure A1. Validation of daily AEROSNOW retrieved AOD colocated with daily AERONET observation AOD obtained over PEARL, OPAL, Hornsund, and Thule stations. The linear regression lines are shown as blue dashed lines.

Code and data availability. The code and data supporting the conclusions of this manuscript are available upon request.

Author contributions. B.S., M.V. conceived the research. B.S. has processed the aerosol data, analyzed all records and wrote the manuscript. S.J. helped in algorithm development. M.V., A.D.,L.L, S.S.G, Y.Z, S.J and J.P.B. helped in shaping this manuscript. Funding acquisition by M.V. and J.P.B. All authors contributed to the interpretation of the results and the final drafting of the paper.

Competing interests. The authors declare that they have no conflict of interest.

Acknowledgements. We thank ESA for AATSR data set. This work has been funded by the Deutsche Forschungsgemeinschaft (DFG, German Research Foundation) within the project "ArctiC Amplification: Climate Relevant Atmospheric and SurfaCe Processes, and Feedback Mechanisms (AC)^3" as Transregional Collaborative Research Center (TRR) 172, Project-ID 268020496.

https://doi.org/10.5194/amt-2023-65
Preprint. Discussion started: 25 April 2023

References

Arimoto, R., Duce, R., Ray, B., Ellis Jr, W., Cullen, J., and Merrill, J.: Trace elements in the atmosphere over the North Atlantic, Journal of Geophysical Research: Atmospheres, 100, 1199–1213, 1995.

Ayers, G.: Comment on regression analysis of air quality data, Atmospheric Environment, 35, 2423–2425, 2001.

Bennartz, R., Shupe, M. D., Turner, D. D., Walden, V., Steffen, K., Cox, C. J., Kulie, M. S., Miller, N. B., and Pettersen, C.: July 2012 Greenland melt extent enhanced by low-level liquid clouds, Nature, 496, 83–86, 2013.

Boisvert, L. N., Petty, A. A., and Stroeve, J. C.: The impact of the extreme winter 2015/16 Arctic cyclone on the Barents–Kara Seas, Monthly Weather Review, 144, 4279–4287, 2016.

Bond, T. C., Doherty, S. J., Fahey, D. W., Forster, P. M., Berntsen, T., DeAngelo, B. J., Flanner, M. G., Ghan, S., Kärcher, B., Koch, D., et al.: Bounding the role of black carbon in the climate system: A scientific assessment, Journal of geophysical research: Atmospheres, 118, 5380–5552, 2013.

Breider, T. J., Mickley, L. J., Jacob, D. J., Ge, C., Wang, J., Payer Sulprizio, M., Croft, B., Ridley, D. A., McConnell, J. R., Sharma, S., et al.: Multidecadal trends in aerosol radiative forcing over the Arctic: Contribution of changes in anthropogenic aerosol to Arctic warming since 1980, Journal of Geophysical Research: Atmospheres, 122, 3573–3594, 2017.

Campen, H. I., Arévalo-Martínez, D. L., Artioli, Y., Brown, I. J., Kitidis, V., Lessin, G., Rees, A. P., and Bange, H. W.: The role of a changing Arctic Ocean and climate for the biogeochemical cycling of dimethyl sulphide and carbon monoxide, Ambio, pp. 1–12, 2022.

Freijer, J. I. and Bloemen, H. J. T.: Modeling relationships between indoor and outdoor air quality, Journal of the Air & Waste Management Association, 50, 292–300, 2000.

Giles, D. M., Sinyuk, A., Sorokin, M. G., Schafer, J. S., Smirnov, A., Slutsker, I., Eck, T. F., Holben, B. N., Lewis, J. R., Campbell, J. R., et al.: Advancements in the Aerosol Robotic Network (AERONET) Version 3 database–automated near-real-time quality control algorithm with improved cloud screening for Sun photometer aerosol optical depth (AOD) measurements, Atmospheric Measurement Techniques, 12, 169–209, 2019.

Glantz, P., Bourassa, A., Herber, A., Iversen, T., Karlsson, J., Kirkevåg, A., Maturilli, M., Seland, Ø., Stebel, K., Struthers, H., et al.: Remote sensing of aerosols in the Arctic for an evaluation of global climate model simulations, Journal of Geophysical Research: Atmospheres, 119, 8169–8188, 2014.

Goosse, H., Kay, J. E., Armour, K. C., Bodas-Salcedo, A., Chepfer, H., Docquier, D., Jonko, A., Kushner, P. J., Lecomte, O., Massonnet, F., et al.: Quantifying climate feedbacks in polar regions, Nature communications, 9, 1–13, 2018.

Hartmann, M., Adachi, K., Eppers, O., Haas, C., Herber, A., Holzinger, R., Hünerbein, A., Jäkel, E., Jentzsch, C., van Pinxteren, M., et al.: Wintertime airborne measurements of ice nucleating particles in the high Arctic: A hint to a marine, biogenic source for ice nucleating particles, Geophysical Research Letters, 47, e2020GL087 770, 2020.

He, M., Hu, Y., Chen, N., Wang, D., Huang, J., and Stamnes, K.: High cloud coverage over melted areas dominates the impact of clouds on the albedo feedback in the Arctic, Scientific reports, 9, 1–11, 2019.

Herber, A., Thomason, L. W., Gernandt, H., Leiterer, U., Nagel, D., Schulz, K.-H., Kaptur, J., Albrecht, T., and Notholt, J.: Continuous day and night aerosol optical depth observations in the Arctic between 1991 and 1999, Journal of Geophysical Research: Atmospheres, 107, AAC–6, 2002.

Hirsch, R. M. and Gilroy, E. J.: METHODS OF FITTING A STRAIGHT LINE TO DATA: EXAMPLES IN WATER RESOURCES 1, JAWRA Journal of the American Water Resources Association, 20, 705–711, 1984.

Hoffmann, A., Osterloh, L., Stone, R., Lampert, A., Ritter, C., Stock, M., Tunved, P., Hennig, T., Böckmann, C., Li, S.-M., et al.: Remote sensing and in-situ measurements of tropospheric aerosol, a PAMARCMiP case study, Atmospheric Environment, 52, 56–66, 2012.

Holben, B. N., Eck, T. F., Slutsker, I. a., Tanre, D., Buis, J., Setzer, A., Vermote, E., Reagan, J. A., Kaufman, Y., Nakajima, T., et al.: AERONET—A federated instrument network and data archive for aerosol characterization, Remote sensing of environment, 66, 1–16, 1998.

Holben, B. N., Tanre, D., Smirnov, A., Eck, T., Slutsker, I., Abuhassan, N., Newcomb, W., Schafer, J., Chatenet, B., Lavenu, F., et al.: An emerging ground-based aerosol climatology: Aerosol optical depth from AERONET, Journal of Geophysical Research: Atmospheres, 106, 12 067–12 097, 2001.

Im, U., Tsigaridis, K., Faluvegi, G., Langen, P. L., French, J. P., Mahmood, R., Thomas, M. A., von Salzen, K., Thomas, D. C., Whaley, C. H., et al.: Present and future aerosol impacts on Arctic climate change in the GISS-E2. 1 Earth system model, Atmospheric Chemistry and Physics, 21, 10 413–10 438, 2021.

Istomina, L., von Hoyningen-Huene, W., Kokhanovsky, A., Schultz, E., and Burrows, J.: Remote sensing of aerosols over snow using infrared AATSR observations, Atmospheric Measurement Techniques, 4, 1133–1145, 2011.

Jafariserajehlou, S., Mei, L., Vountas, M., Rozanov, V., Burrows, J. P., and Hollmann, R.: A cloud identification algorithm over the Arctic for use with AATSR–SLSTR measurements, Atmospheric Measurement Techniques, 12, 1059–1076, 2019.

Kapsch, M.-L., Graversen, R. G., and Tjernström, M.: Springtime atmospheric energy transport and the control of Arctic summer sea-ice extent, Nature Climate Change, 3, 744–748, 2013.

Kato, S., Loeb, N. G., Minnis, P., Francis, J. A., Charlock, T. P., Rutan, D. A., Clothiaux, E. E., and Sun-Mack, S.: Seasonal and interannual variations of top-of-atmosphere irradiance and cloud cover over polar regions derived from the CERES data set, Geophysical Research Letters, 33, 2006.

Kaufman, Y. J. and Fraser, R. S.: The effect of smoke particles on clouds and climate forcing, Science, 277, 1636–1639, 1997.

Keene, W. C., Pszenny, A. A., Galloway, J. N., and Hawley, M. E.: Sea-salt corrections and interpretation of constituent ratios in marine precipitation, Journal of Geophysical Research: Atmospheres, 91, 6647–6658, 1986.

Kokhanovsky, A. A. and Breon, F.-M.: Validation of an analytical snow BRDF model using PARASOL multi-angular and multispectral observations, IEEE Geoscience and Remote Sensing Letters, 9, 928–932, 2012.

Llewellyn-Jones, D., Edwards, M., Mutlow, C., Birks, A., Barton, I., and Tait, H.: AATSR: Global-change and surface-temperature measurements from Envisat, ESA bulletin, 105, 25, 2001.

Mei, Rozanov, V., Ritter, C., Heinold, B., Jiao, Z., Vountas, M., and Burrows, J. P.: Retrieval of aerosol optical thickness in the Arctic snow-covered regions using passive remote sensing: impact of aerosol typing and surface reflection model, IEEE Transactions on Geoscience and Remote Sensing, 58, 5117–5131, 2020a.

Mei, L., Xue, Y., de Leeuw, G., von Hoyningen-Huene, W., Kokhanovsky, A. A., Istomina, L., Guang, J., and Burrows, J. P.: Aerosol optical depth retrieval in the Arctic region using MODIS data over snow, Remote Sensing of Environment, 128, 234–245, 2013.

Mei, L., Vandenbussche, S., Rozanov, V., Proestakis, E., Amiridis, V., Callewaert, S., Vountas, M., and Burrows, J. P.: On the retrieval of aerosol optical depth over cryosphere using passive remote sensing, Remote Sensing of Environment, 241, 111 731, https://doi.org/https://doi.org/10.1016/j.rse.2020.111731, 2020b.

Mei, L., Rozanov, V., Rozanov, A., and Burrows, J. P.: SCIATRAN software package (V4.6): update and further development of aerosol, clouds, surface reflectance databases and models, Geoscientific Model Development, 16, 1511–1536, https://doi.org/10.5194/gmd-16-1511-2023, 2023.

Middlemas, E., Kay, J., Medeiros, B., and Maroon, E.: Quantifying the influence of cloud radiative feedbacks on Arctic surface warming using cloud locking in an Earth system model, Geophysical Research Letters, 47, e2020GL089 207, 2020.

Moschos, V., Schmale, J., Aas, W., Becagli, S., Calzolai, G., Eleftheriadis, K., Moffett, C. E., Schnelle-Kreis, J., Severi, M., Sharma, S., et al.: Elucidating the present-day chemical composition, seasonality and source regions of climate-relevant aerosols across the Arctic land surface, Environmental Research Letters, 17, 034 032, 2022.

Nakoudi, K., Ritter, C., Neuber, R., and Müller, K. J.: Optical Properties of Arctic Aerosol during PAMARCMiP 2018, 2018.

Nummelin, A., Li, C., and Hezel, P. J.: Connecting ocean heat transport changes from the midlatitudes to the Arctic Ocean, Geophysical Research Letters, 44, 1899–1908, 2017.

Ohata, S., Koike, M., Yoshida, A., Moteki, N., Adachi, K., Oshima, N., Matsui, H., Eppers, O., Bozem, H., Zanatta, M., et al.: Arctic black carbon during PAMARCMiP 2018 and previous aircraft experiments in spring, Atmospheric Chemistry and Physics, 21, 15 861–15 881, 2021.

Park, J.-Y., Kug, J.-S., Bader, J., Rolph, R., and Kwon, M.: Amplified Arctic warming by phytoplankton under greenhouse warming, Proceedings of the National Academy of Sciences, 112, 5921–5926, 2015.

Perovich, D. K. and Polashenski, C.: Albedo evolution of seasonal Arctic sea ice, Geophysical Research Letters, 39, 2012.

Pithan, F. and Mauritsen, T.: Arctic amplification dominated by temperature feedbacks in contemporary climate models, Nature geoscience, 7, 181–184, 2014.

Popp, T., De Leeuw, G., Bingen, C., Brühl, C., Capelle, V., Chedin, A., Clarisse, L., Dubovik, O., Grainger, R., Griesfeller, J., Heckel, A., Kinne, S., Klüser, L., Kosmale, M., Kolmonen, P., Lelli, L., Litvinov, P., Mei, L., North, P., Pinnock, S., Povey, A., Robert, C., Schulz, M., Sogacheva, L., Stebel, K., Stein Zweers, D., Thomas, G., Tilstra, L. G., Vandenbussche, S., Veefkind, P., Vountas, M., and Xue, Y.: Development, Production and Evaluation of Aerosol Climate Data Records from European Satellite Observations (Aerosol_cci), Remote Sensing, 8, https://doi.org/10.3390/rs8050421, 2016.

Riggs, G. A., Hall, D. K., and Román, M. O.: Overview of NASA's MODIS and visible infrared imaging radiometer suite (VIIRS) snow-cover earth system data records, Earth System Science Data, 9, 765–777, 2017.

Rozanov, Rozanov, A., Kokhanovsky, A. A., and Burrows, J.: Radiative transfer through terrestrial atmosphere and ocean: Software package SCIATRAN, Journal of Quantitative Spectroscopy and Radiative Transfer, 133, 13–71, 2014.

Rozanov, A.: Modeling of radiative transfer through a spherical planetary atmosphere: Application to atmospheric trace gases retrieval from occultation-and limb-measurements in UV-Vis-NIR, Ph.D. thesis, Universität Bremen, 2001.

Rozanov, A., Rozanov, V., Buchwitz, M., Kokhanovsky, A., and Burrows, J.: SCIATRAN 2.0–A new radiative transfer model for geophysical applications in the 175–2400 nm spectral region, Advances in Space Research, 36, 1015–1019, 2005.

Rozanov, V., Buchwitz, M., Eichmann, K.-U., De Beek, R., and Burrows, J.: SCIATRAN-a new radiative transfer model for geophysical applications in the 240–2400 nm spectral region: The pseudo-spherical version, Advances in Space Research, 29, 1831–1835, 2002.

Sand, M., Samset, B. H., Balkanski, Y., Bauer, S., Bellouin, N., Berntsen, T. K., Bian, H., Chin, M., Diehl, T., Easter, R., et al.: Aerosols at the poles: an AeroCom Phase II multi-model evaluation, Atmospheric Chemistry and Physics, 17, 12 197–12 218, 2017.

Schmale, J., Sharma, S., Decesari, S., Pernov, J., Massling, A., Hansson, H.-C., Von Salzen, K., Skov, H., Andrews, E., Quinn, P. K., et al.: Pan-Arctic seasonal cycles and long-term trends of aerosol properties from 10 observatories, Atmospheric Chemistry and Physics, 22, 3067–3096, 2022.

Serreze, M. C. and Francis, J. A.: The Arctic amplification debate, Climatic change, 76, 241–264, 2006.

https://doi.org/10.5194/amt-2023-65
Preprint. Discussion started: 25 April 2023

Sinyuk, A., Holben, B. N., Smirnov, A., Eck, T. F., Slutsker, I., Schafer, J. S., Giles, D. M., and Sorokin, M.: Assessment of error in aerosol optical depth measured by AERONET due to aerosol forward scattering, Geophysical Research Letters, 39, 2012.

Stapf, J., Ehrlich, A., Jäkel, E., Lüpkes, C., and Wendisch, M.: Reassessment of shortwave surface cloud radiative forcing in the Arctic: consideration of surface-albedo–cloud interactions, Atmospheric Chemistry and Physics, 20, 9895–9914, 2020.

Tomasi, C., Vitale, V., Lupi, A., Di Carmine, C., Campanelli, M., Herber, A., Treffeisen, R., Stone, R., Andrews, E., Sharma, S., et al.: Aerosols in polar regions: A historical overview based on optical depth and in situ observations, Journal of Geophysical Research: Atmospheres, 112, 2007.

Toth, T. D., Campbell, J. R., Reid, J. S., Tackett, J. L., Vaughan, M. A., Zhang, J., and Marquis, J. W.: Minimum aerosol layer detection sensitivities and their subsequent impacts on aerosol optical thickness retrievals in CALIPSO level 2 data products, Atmospheric Measurement Techniques, 11, 499–514, 2018.

Twomey, S.: The influence of pollution on the shortwave albedo of clouds, Journal of the atmospheric sciences, 34, 1149–1152, 1977.

Vermote, E., El Saleous, N., Justice, C., Kaufman, Y., Privette, J., Remer, L., Roger, J.-C., and Tanre, D.: Atmospheric correction of visible to middle-infrared EOS-MODIS data over land surfaces: Background, operational algorithm and validation, Journal of Geophysical Research: Atmospheres, 102, 17 131–17 141, 1997.

Wang, T., Wong, C., Cheung, T., Blake, D., Arimoto, R., Baumann, K., Tang, J., Ding, G., Yu, X., Li, Y. S., et al.: Relationships of trace gases and aerosols and the emission characteristics at Lin'an, a rural site in eastern China, during spring 2001, Journal of Geophysical Research: Atmospheres, 109, 2004.

Wendisch, M., Macke, A., Ehrlich, A., Lüpkes, C., Mech, M., Chechin, D., Dethloff, K., Velasco, C. B., Bozem, H., Brückner, M., et al.: The Arctic cloud puzzle: Using ACLOUD/PASCAL multiplatform observations to unravel the role of clouds and aerosol particles in Arctic amplification, Bulletin of the American Meteorological Society, 100, 841–871, 2019.

Willis, M. D., Leaitch, W. R., and Abbatt, J. P.: Processes controlling the composition and abundance of Arctic aerosol, Reviews of Geophysics, 56, 621–671, 2018.

Winker, D. M., Hunt, W. H., and Hostetler, C. A.: Status and performance of the CALIOP lidar, in: Laser Radar Techniques for Atmospheric Sensing, vol. 5575, pp. 8–15, SPIE, 2004.

Wu, C., Xian, Z., and Huang, G.: Meteorological drought in the Beijiang River basin, South China: current observations and future projections, Stochastic environmental research and risk assessment, 30, 1821–1834, 2016.

Xian, P., Zhang, J., Toth, T. D., Sorenson, B., Colarco, P. R., Kipling, Z., O'Neill, N. T., Hyer, E. J., Campell, J. R., Reid, J. S., et al.: Arctic spring and summertime aerosol optical depth baseline from long-term observations and model reanalyses, with implications for the impact of regional biomass burning processes, Atmospheric Chemistry and Physics Discussions, pp. 1–63, 2021.